

## Alternatives for understanding qualitative features that dominate particle-particle correlations in heavy-ion reactions of $\approx 50$ MeV/nucleon

John M. Alexander,<sup>1</sup> A. Elmaani,<sup>1,\*</sup> L. Kowalski,<sup>2</sup> N. N. Ajitanand,<sup>1</sup> and C. J. Gelderloos<sup>1</sup>

<sup>1</sup>*Departments of Chemistry and Physics, State University of New York at Stony Brook,  
Stony Brook, New York 11794*

<sup>2</sup>*Department of Physics and Geoscience, Montclair State College, Upper Montclair, New Jersey 07043*

(Received 24 May 1993)

We use trajectory calculations to analyze small-angle particle-particle correlations for three typical situations:  $^{40}\text{Ar} + ^{197}\text{Au}$  ( $E/A=60$  MeV)  $\rightarrow$   $^2\text{H}$ - $^2\text{H}$  pairs and  $^1\text{H}$ - $^1\text{H}$  pairs,  $^{20}\text{Ne} + ^{59}\text{Cu}$  ( $E/A = 30$  MeV)  $\rightarrow$  n-n pairs. For the  $^2\text{H}$ - $^2\text{H}$  pairs our analysis of the gentle featureless anticorrelations suggests that the major driving force is Coulomb repulsion after a range of average time delays from  $\approx 5 \times 10^{-21}$  s for the  $^2\text{H}$  pairs of lower energy to  $\approx 10^{-22}$  s for the  $^2\text{H}$  pairs of higher energy. Simulations are used to illustrate the separate dominance of source size and lifetime in the space-time extent of the emitter. For lifetimes  $\leq 10^{-22}$  s the emitter size dominates; for longer lifetimes the time delays become predominant. The peaks at  $\approx 20$  MeV/c in the correlation functions for  $^1\text{H}$ - $^1\text{H}$  pairs can be accounted for by diproton ejection which decays into protons with a  $Q$  value of  $\approx 0.35$  MeV and a decay width of  $\approx 1$  MeV (or a meanlife of  $6 \times 10^{-22}$  s). The positive correlations between neutron pairs can be accounted for by dineutron ejection which decays into neutrons with a near zero  $Q$  value and a decay width of  $\approx 0.25$  MeV (or a meanlife of  $\approx 2 \times 10^{-21}$  s). If these diproton and dineutron clusters do indeed have a metastable existence, then one should reexamine the notion that their associated small-angle correlations reflect the space-time extent of the emission source.

PACS number(s): 25.70.Pq

### I. INTRODUCTION

Many studies of heavy-ion-induced nuclear reactions at near-barrier energies ( $\leq 10$  MeV/nucleon) have indicated the formation of a thermalized compound nuclear system which decays by particle evaporation or fission on a time scale of  $\geq 10^{-21}$  s ( $\geq 300$  fm/c) [1]. By contrast, central collisions of heavy ions at relativistic energies ( $\geq 1000$  MeV/nucleon) generally involve much more energy density than the nuclear binding can contain, and hence lead to explosive nuclear expansion on a time scale of a few fm/c [2]. A feature of great interest in these latter reactions is the magnitude of the energy density in the reaction zone. Thus there has been great interest in the characterization of the size of this reaction zone, and a number of papers have addressed the use of particle interferometry for this purpose (i.e., small-angle particle-particle correlations). (See, for example, [3,4] and many references therein.)

The main feature, interest, and utility of particle interferometry in this context is for reactions with intrinsic time delays of only a few fm/c. Hence, for these nearly instantaneous explosions the major driving forces for the particle-particle correlations are nurtured by the small volume of their place of birth [3,4]. The situation is quite different for those reactions involving much smaller en-

ergy densities, which can be thermalized into nucleonic motion and contained by the nuclear binding in a long lived compound nucleus. Although these compound nuclei may be somewhat swollen [5], the small-angle correlations between successively emitted particles are driven by final state interactions over distances essentially determined by the rather long time delays (typically  $\geq 300$  fm/c) between emissions [6]. Here interpretations can be made by using reaction simulations that employ trajectory calculations dominated by three-body Coulomb interactions (see, for example, [7]).

The most difficult situations to understand lie between these limits of low and high energies, i.e., for intermediate incident energies ( $\approx 20$ – $200$  MeV/nucleon) where one cannot be sure *a priori* if compound nuclei are formed or if there is a single explosive expansion followed by “droplet condensation” [4,8]. The formation mechanism for nucleonic clusters and intermediate-mass fragments (IMF’s) is one crucial aspect for our understanding of this transition energy region [9]. It is clear from studies at near-barrier energies that such nuclear fragments of mass number 2–20 are produced as evaporated particles or asymmetric fissionlike fragments in successive decay steps from a hot compound nucleus [10–12]. These mechanisms are very different from the thermal model described in [8]. It is not clear exactly how these complex particle and/or fragment emissions change as one increases the incident heavy-ion energy from units to tens to hundreds of MeV per nucleon.

In this study we try to develop some insights into this transition energy region by comparing reaction simulation calculations to several typical data sets taken from

\*Present address: University of Washington, Nuclear Physics Lab GL-10, Seattle, WA 98195.

the literature. The reactions we choose are  $^{40}\text{Ar}$  ( $E/A = 60$  MeV) +  $^{197}\text{Au} \rightarrow {}^2\text{H}\text{-}^2\text{H}$  pairs or  ${}^1\text{H}\text{-}^1\text{H}$  pairs [13] and  $^{20}\text{Ne}$  ( $E/A = 30$  MeV) +  $^{59}\text{Co} \rightarrow {}^1n\text{-}^1n$  pairs [14]. In each case particle-particle coincidence measurements were made at  $\approx 30^\circ$  in the laboratory; the energy spectra include very energetic particles that must come from prethermalization emission and not from statistical evaporation. For situations similar to these, serious questions have been raised [15,16] concerning the applicability of the often-used models for interpreting such data. We use trajectory calculations to get some general ideas about the mechanisms and interparticle distances involved, and we explore the possible roles of dinucleonic systems—deuterons, diprotons [17], and dineutrons. It is not our intent to suggest that these classical calculations can give precise or definitive interpretations. But we do feel that they can suggest important features that may well be decisive for a qualitative understanding and hence for a more detailed model.

## II. TRAJECTORY CALCULATIONS FOR PRETHERMALIZATION EMISSION

Heavy-ion reactions often result in the preferential emission of particles in the forward direction (i.e., along the general direction of the lighter collision partner) with a wide spectrum of energies (see, e.g., [18]). The particle spectra often change with angle and have higher spectral temperatures at more forward angles. A significant fraction of the forward particles is said to be emitted prior to thermal equilibration (i.e., prethermalization emission). Since energy thermalization among the nucleons occurs on a very fast scale  $\approx 10^{-22}$  s [19], one can expect that such prethermalization emission involves the early phase of the nucleonic collision cascade and thus the first several steps in composite nuclear deexcitation.

In the reaction simulation code MENEKA [6], we have developed an option to consider these more or less direct reactions. As in other options the time intervals between the emission of particles are assumed to be distributed exponentially, but here the mean decay times are calculated as follows:

$$\tau \approx S \left( \frac{R}{V_1} - \frac{R}{V_2} \right).$$

The symbols  $V_1$  and  $V_2$  represent velocities of the two particles,  $R$  is the radius of the struck nucleus, and  $S$  is an adjustable scaling factor, normally set to a value close to unity. The decay times are thus determined directly from the energies of selected particles (as differences between the nominal traversal times), and the values are typically  $\approx 10^{-22}$  s. Other aspects of the simulation are exactly the same as previously described [7]. The idea here is to apply the trajectory approach to high-energy forward-peaked particles to get a feeling for the characteristic times and distances involved in their production. In the next section we will present results obtained by using this method to fit some typical experimental results from the literature.

## III. ILLUSTRATIVE DISCUSSION FOR ${}^2\text{H}\text{-}^2\text{H}$ PAIRS FROM DIRECT REACTIONS

To explore this picture of direct prethermalization emission, as implemented in the code MENEKA, we have first selected a set of experimental data for the reaction of 2400 MeV  $^{40}\text{Ar} + {}^{197}\text{Au} \rightarrow {}^2\text{H}\text{-}^2\text{H}$  pairs [13]. The experimenters used a cluster of small detectors placed in the forward hemisphere centered at  $\theta_{\text{lab}} \approx 30^\circ$ . Acceptance geometry was introduced in the simulation to mimic the granularity of the detectors used. The authors give an analytical expression for the spectral shapes in which three Maxwellian distributions are superposed to generate the energy spectrum of the observed particle. The resulting energy spectrum is shown in Fig. 1(a) (square symbols); a “fit” of this spectrum, using a more simple formula in MENEKA is shown in the same figure (crosses). This fit leaves something to be desired, but it is adequate for the points that we wish to make here. The summed energy in the laboratory for each coincident pair of deuterons,  $E_{\text{tot}}$ , is shown in Fig. 1(b).

After selecting the energies of a given  ${}^2\text{H}\text{-}^2\text{H}$  particle

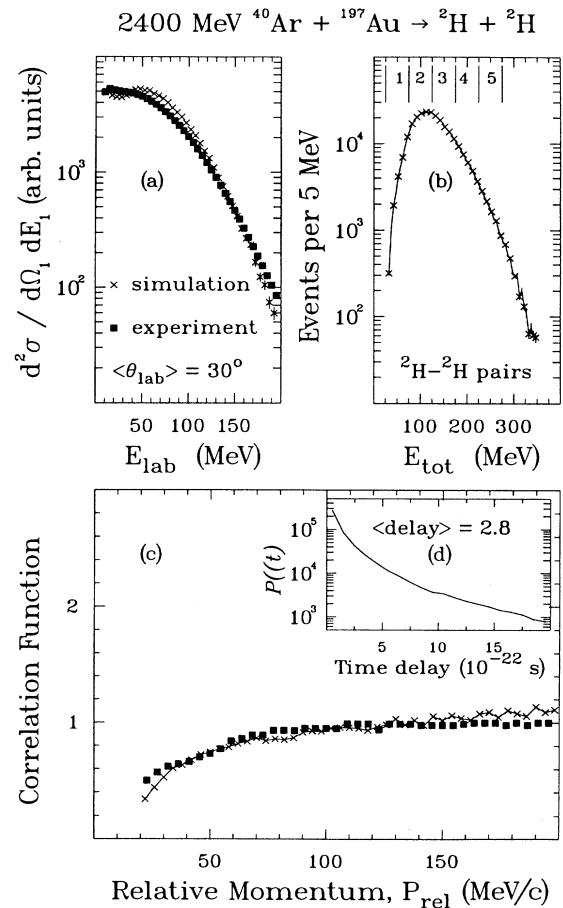


FIG. 1. (a) Experimental and calculated energy spectra. (b) Summed laboratory energy spectrum. (c) Experimental and calculated correlation functions. (d) Emission time delay distribution for 2400 MeV  $^{40}\text{Ar} + ^{197}\text{Au} \rightarrow {}^2\text{H}\text{-}^2\text{H}$ . Crosses refer to results of simulations.

pair, MENEKA calculates the emission time delay event by event from the procedure described above in Sec. II. A trajectory calculation is then carried out including Coulomb forces (for the three-body system) and nuclear forces (between the two ejectiles [20]). After some exploration, the time size scale factor  $S$  was set to 1.7 to get a fit to the correlation function. Both the experimental as well as the calculated correlation functions are given in Fig. 1(c). A time distribution or decay curve which results from this treatment is shown in Fig. 1(d); for the chosen scale factor the time delay for these emissions is ( $\approx 2.8 \times 10^{-22}$  s). The calculated correlation function compares rather well to the data, but is somewhat too small for small values of  $P_{\text{rel}}$ . A reason for this discrepancy becomes apparent below, in the discussion of  $\tau$  values required for the energy gated correlation functions.

We test this approach in more detail by fitting the experimental correlation functions obtained with constraints imposed on the summed energy of the two deuterons. The ranges of interest are labeled 1, 2, 3, 4, and 5 in Fig. 1b, and the corresponding observed and calculated correlation functions are shown in Fig. 2. For the lowest-energy gate,  $25 \leq E_{\text{tot}} \leq 75$  MeV, a large scale factor  $S \approx 20$  is required to obtain a fit to the experimental correlation function. The average time delay

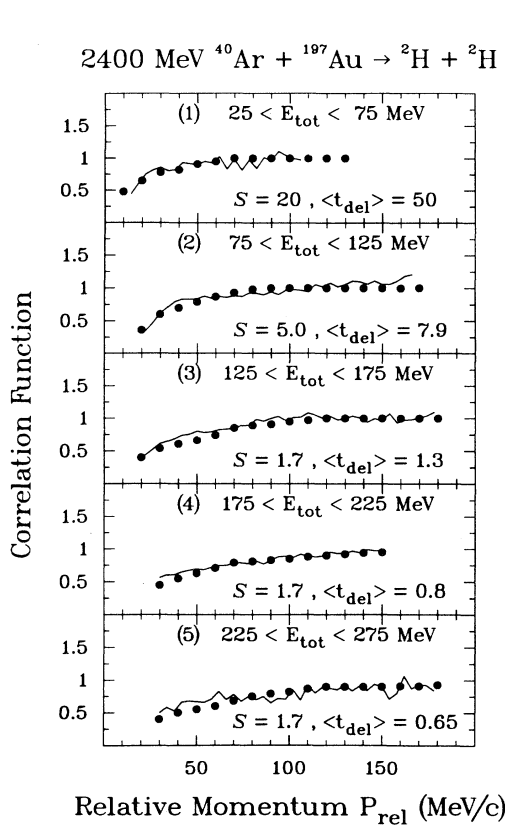


FIG. 2. Five experimental and calculated correlation functions corresponding to different ranges for the total laboratory energy of  $^2\text{H}$ - $^2\text{H}$  pairs from  $2400 \text{ MeV } ^{40}\text{Ar} + ^{197}\text{Au} \rightarrow ^2\text{H}$ - $^2\text{H}$ . Relative contributions for the ranges, labeled 1, 2, 3, 4, or 5 can be seen in Fig. 1(b).

for this energy gate was found to be  $\langle t_{\text{del}} \rangle \approx 50.5 \times 10^{-22}$  s. Such a large time delay seems to indicate an extensive time for energy mixing; hence the low-energy particles seem to be evaporated from sources that are much more extensively thermalized than the average [21].

For the next energy gate,  $75 \leq E_{\text{tot}} \leq 125$  MeV, the experimental correlation function is fit with an intermediate scale factor  $S \approx 5$  that produces an average time delay of  $7.9 \times 10^{-22}$  s. Finally for the higher-energy gates,  $125 \leq E_{\text{tot}} \leq 175$  MeV,  $175 \leq E_{\text{tot}} \leq 225$  MeV, and  $225 \leq E_{\text{tot}} \leq 275$  MeV, the original scale factor of  $S = 1.7$  is found to give a reasonable fit to the experimental correlation functions. The respective average time delays for the last three gates have a range but are similar to that for the ungated correlation function. These calculated fits using MENEKA are consistent with one's intuitive expectation; i.e., the faster processes are associated with higher energies of the emitted particles. Also this wide range of  $\tau$  values accounts for the failure to achieve a good fit in Fig. 1 with only a single  $\tau$  value of the scale factor.

A point of major significance for our understanding of such results is the relative importance of time delay vs nuclear size as the main cause for the particle-particle correlations [4,21–25]. In Fig. 3 we illustrate this point

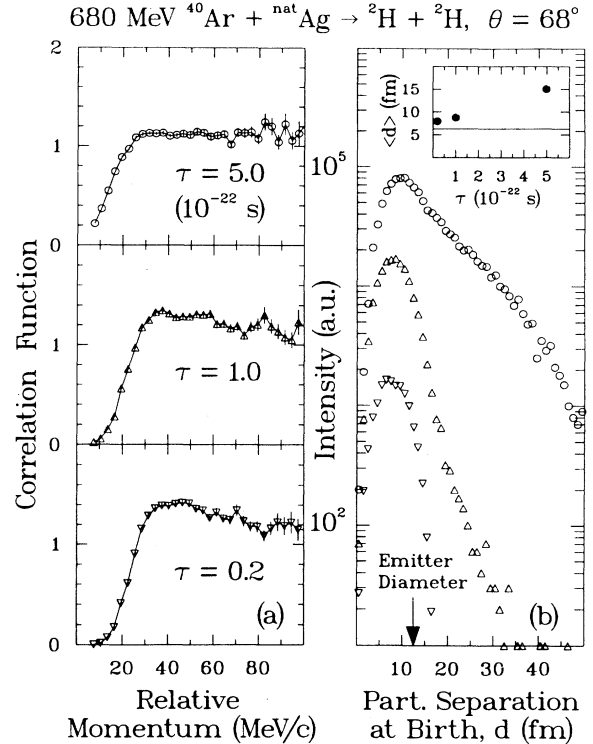


FIG. 3. (a) Calculated correlation functions and (b) spectra of  $^2\text{H}$ - $^2\text{H}$  separation distances for three different mean lifetimes  $\tau$  of the emitter ( $\tau = 5.0, 1.0$ , and  $0.2 \times 10^{-22}$  s or 150, 30, and 6 fm/c). The inset shows the average separation distance vs  $\tau$  compared to a horizontal line at the emitter radius. For  $\tau \leq 0.2 \times 10^{-22}$  s the spectrum of separation distances is essentially independent of  $\tau$  and reflects only the random choices of birthplace on the emitter surface.

by showing calculated correlation functions along with spectra of the initial separation distance between two  ${}^2\text{H}$  particles in the exit channel. For these simulations of the  ${}^{40}\text{Ar} + \text{Ag}$  reaction [25] the birthplace of the first  ${}^2\text{H}$  particle is chosen at random on the emitter surface [7]. Then the time delay before the second  ${}^2\text{H}$  emission is chosen at random from an exponential decay function with mean lifetime  $\tau$ . During this period the first particle is accelerated along a two-body Coulomb trajectory. The birthplace of the second  ${}^2\text{H}$  particle is then chosen at random on the emitter surface, and a three-body trajectory calculation is initiated. Therefore, the particle separation distances (at birth of the second particle) in Fig. 3 result from addition of the flight distance of the first particle plus the distance between randomly selected birth places. For the smallest  $\tau$  value ( $0.2 \times 10^{-22}$  s or 6 fm/c) the latter distance dominates because the flight paths are negligible. Clearly for such short  $\tau$  values only the emitter size is important. For  $\tau = 1 \times 10^{-22}$  s one also has only a small effect of flight path, but for  $\tau = 5 \times 10^{-22}$  s (or 150 fm/c) the spectrum shows a clear influence of the flight times.

The message of Fig. 3 is that for time delays of  $< 5 \times 10^{-22}$  s (or 150 fm/c) the intrinsic emitter size will begin to be significant for the closest interparticle separation distances and hence their exit channel interactions. Indeed, in our calculations leading to Fig. 1, the calculated correlation functions lose sensitivity to the scale factor for  $S$  values less than unity. We conclude that the time delay dominates the correlation functions for mean lifetimes  $\geq 5 \times 10^{-22}$  s; the emitter size dominates for  $\leq 10^{-22}$  s, and both play a role for  $\approx 1-5 \times 10^{-22}$  s. For the case illustrated in Figs. 1 and 2 ( $2400 \text{ MeV } {}^{40}\text{Ar} + {}^{197}\text{Au} \rightarrow {}^2\text{H}, {}^2\text{H}$  pairs), one clearly has prethermalization emission, but nevertheless the time delays seem to be most important for the correlation function.

#### IV. CORRELATIONS BETWEEN ${}^1\text{H}$ - ${}^1\text{H}$ PAIRS: ANOTHER LOOK AT ${}^2\text{He}$

In [13] correlation measurements were presented for  ${}^1\text{H}$ - ${}^1\text{H}$  pairs along with the  ${}^2\text{H}$ - ${}^2\text{H}$  pairs discussed above. The results shown in Fig. 4 for  ${}^1\text{H}$ - ${}^1\text{H}$  pairs have a qualitatively different pattern compared to Fig. 2 for  ${}^2\text{H}$ - ${}^2\text{H}$  pairs. For deuterons there is only a gentle featureless anticorrelation for the smaller relative momenta; however, for protons there is broad peak for  $P_{\text{rel}}$  values of  $\approx 20 \text{ MeV}/c$ . This peak is generally attributed to the role of short-range attractive nuclear forces between the protons [4]. Indeed, calculations with the Koonin model [24] can often reproduce such data by invoking effective emitter radii of  $\approx 6 \text{ fm}$  (see, e.g., [15,16], and references therein). For reactions at much lower incident energies these peaks disappear from the  ${}^1\text{H}$ - ${}^1\text{H}$  correlations and only anticorrelations are found that are qualitatively similar to those in Figs. 1 and 2 for  ${}^2\text{H}$  [6,22,25,26]. This behavior change is attributed to longer time intervals between proton emissions from relatively cooler composite nuclei.

Some time ago Bernstein *et al.* [17] reported that it was

possible to account for the characteristic peak in proton correlation functions by invoking evaporation of diproton entities (or  ${}^2\text{He}$ ). They reexamined proton-proton scattering data to obtain  $Q$  values and resonance widths ( $W$ ) for  ${}^2\text{He}$ ; then they used these properties in trajectory calculations that included isotropic  ${}^2\text{He}$  breakup after a long flight path for escape from the hot emitter. (Recently we have made similar calculations for correlations between  ${}^4\text{He}$ - ${}^4\text{He}$  pairs generated by the decay of unstable  ${}^8\text{Be}$  [25,26].) For such a mechanism it is likely that the small-angle particle correlations lose all information content on the space-time extent of the source. Instead, the major contributing factor for the correlation function peaks would be the relative yield of the emitted cluster, i.e., for  ${}^2\text{He}$  (or  ${}^8\text{Be}$ ) versus the yield of independently emitted proton pairs (or  $\alpha$ -particle pairs).

We wish to follow up on this idea from [17] with two main differences in the trajectory calculations: (a) We leave the values of  $Q$  and  $W$  for  ${}^2\text{He}$  as free parameters to be constrained by fits to the correlation functions. (b) We assign individual decay times to each emitted  ${}^2\text{He}$  entity based on exponential decay of a state in  ${}^2\text{He}$  of width  $W$ . The associated three-body trajectories are then calculated including the effect of the residual nucleus as well as the two protons [6].

The smooth curves in Fig. 4 show results of such calculations compared to the experimental data (solid

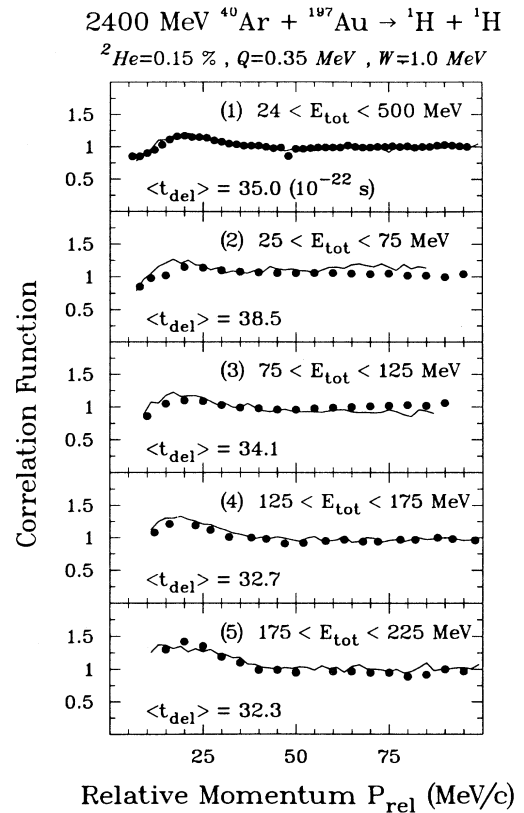


FIG. 4. Five experimental and calculated correlation functions for  ${}^1\text{H}$ - ${}^1\text{H}$  pairs corresponding to different ranges for the total laboratory energy.

circles). Various input parameters are indicated at the top of the figure. The position of the correlation peak ( $P_{\text{rel}} \approx 20 \text{ MeV}/c$ ) dictates the  $Q$  value of  $0.35 \pm 0.05$  for the decay energy. The width of the peak leads to an assignment of  $W = 1 \pm 0.3 \text{ MeV}$ . The strength of the peak leads to a relative yield of  $0.15\% \pm 0.04\%$   ${}^2\text{He}$  versus independent  ${}^1\text{H}$  pairs. The shape of the correlation function for those  ${}^1\text{H}$ - ${}^1\text{H}$  pairs with very small ( $P_{\text{rel}}$ ) is consistent with delay times of  $\approx 3 \times 10^{-21} \text{ s}$  between the independently emitted protons. None of these parameters is unacceptable or inconsistent with relevant data from other experiments [17,27,28].

In this analysis of the data, one has invoked the direct ejection of  ${}^2\text{He}$ , albeit with very low probability compared to its cousin  ${}^2\text{H}$ . The only difference is that the  ${}^2\text{He}$  has a decay width of ( $\approx 1 \text{ MeV}$ ) or mean lifetime of  $\approx 6 \times 10^{-22} \text{ s}$  while  ${}^2\text{H}$  is stable. With such a mean lifetime the average flight path of the  ${}^2\text{He}$  clusters would be ( $\approx 18 \text{ fm}$ ). Such a mean lifetime and flight path would seem to be long enough to allow one to think of the  ${}^2\text{He}$  object as possessing the capability for an independent existence. It is this independent existence that is a requirement for the trajectory picture to have some pedagogical merit. In short, we find that we agree with Bernstein *et al.* [17] that there is a possibility that an important feature of proton-proton correlation measurements may well be the yield of  ${}^2\text{He}$  production compared to that for independent proton production.

## V. CORRELATIONS BETWEEN NEUTRONS: POSSIBLY A LOOK AT DINEUTRONS

Recently Jakobsson *et al.* [14] have presented a study of small-angle correlations between neutron pairs from reactions of  $30 \text{ MeV/nucleon } {}^{20}\text{Ne}$  with  ${}^{59}\text{Co}$  and  ${}^{12}\text{C}$ . The results, as shown in Fig. 5(c) for  ${}^{59}\text{Co}$ , exhibit a very positive correlation for very small values of the relative momenta. This positive correlation can be attributed to nuclear attractive forces that are much more effective than for  ${}^1\text{H}$ - ${}^1\text{H}$  pairs due to the absence of Coulomb repulsions [4]. It has long been speculated that these attractive forces might lead to the existence of a stable or metastable dineutron entity [28,29]. However, there has been no experimental confirmation for the existence of such dineutrons. In this section we reanalyze the data from Ref. [14] with the approach used in Sec. IV above. We seek a fit to the experimental correlation functions for neutron pairs by varying the parameters  $Q$  and  $W$  for the hypothetical dineutrons.

The solid curve in Fig. 5(c) shows results of such calculations compared to the experimental data. Input parameters are indicated on the figure. The near-zero value for  $Q$  comes from the increasingly strong correlation for decreasing ( $P_{\text{rel}}$ ) values (no peak was identified). The shape of this curve leads to an assignment of ( $W = 0.25 \pm 0.08 \text{ MeV}$ ) along with a yield of ( $1.2 \pm 0.4\%$ ) compared to independently produced neutron pairs. We have no experimental criterion for assigning the mean delay time between the independently produced neutrons, and so we have used the value  $\tau = 50 \times 10^{-22} \text{ s}$  from earlier work (it

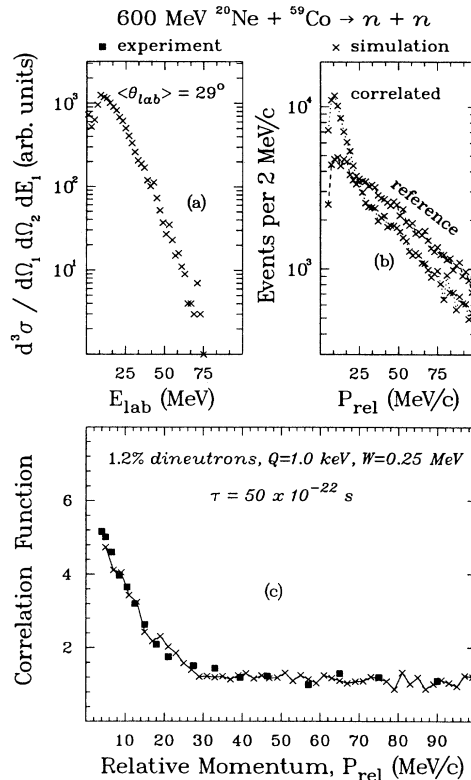


FIG. 5. (a) Simulated energy spectrum. (b) Simulated relative momentum ( $P_{\text{rel}}$ ) spectra for real or correlated events and for reference or uncorrelated events. (c) Experimental and simulated correlation functions for  $600 \text{ MeV } {}^{20}\text{Ne} + {}^{59}\text{Co} \rightarrow n-n$  pairs.

is actually not of major importance). In Figs. 5(a) and 5(b) we show the energy spectrum used for the simulations of independently emitted neutrons. The simulated  $P_{\text{rel}}$  spectra (real and reference) are, of course, very sensitive to the shape of the input energy spectrum. However, the capability to fit the correlation function is not very dependent on this input energy spectrum. Only small changes in the values of the dineutron parameters can compensate for wide swings in the shape of the neutron energy spectra.

In this trajectory calculation one has invoked the metastable existence of a dineutron entity with decay width of ( $\approx 0.25 \text{ MeV}$ ) or mean lifetime of  $\approx 2 \times 10^{-21} \text{ s}$ . If this analysis has even qualitative validity, it could have important significance for the interpretation of  $n-n$  correlation data as well as for the theory of two-nucleon systems (see, for example, [29,30]).

## VI. SUMMARY AND CONCLUSIONS

We have used trajectory calculations to analyze typical experimental data from the literature on small-angle correlations between  ${}^2\text{H}$ - ${}^2\text{H}$  pairs,  ${}^1\text{H}$ - ${}^1\text{H}$  pairs, and  $n-n$  pairs. The experiments employed  ${}^{20}\text{Ne}$  and  ${}^{40}\text{Ar}$  beams of  $30A$  and  $60A$  MeV and made observations of high-

energy particles at  $\approx 30^\circ$  in the laboratory. For the  ${}^2\text{H}-{}^2\text{H}$  pairs we show that trajectory calculations give a good account for the data with average delay times of only  $\approx 2.8 \times 10^{-22}$  s between independently emitted deuterons. For  ${}^1\text{H}-{}^1\text{H}$  pairs the correlation functions have broad peaks for  $P_{\text{rel}} \approx 20 \text{ MeV}/c$  in contrast to the featureless anticorrelations for  ${}^2\text{H}-{}^2\text{H}$  pairs. These peaks can be accounted for by a very small yield of metastable  ${}^2\text{He}$  if its decay into two protons is characterized by a  $Q$  value of  $\approx 0.35 \text{ MeV}$  and a meanlife of  $\approx 0.6 \times 10^{-21}$  s. For neutron pairs the correlation function increases strongly with decreasing  $P_{\text{rel}}$  values down to the experimental threshold of  $\approx 4 \text{ MeV}/c$ . This behavior can be accounted for by a small yield of a metastable dineutron

if its decay into two neutrons is characterized by a  $Q$  value near to zero and mean lifetime of  $\approx 2 \times 10^{-21}$  s. If these suggestions have qualitative merit, they can have an important influence on our approach to extracting information from studies of particle-particle correlations.

#### ACKNOWLEDGMENTS

B. Noren has been very helpful to us concerning details of the work in Ref. [14]. Financial support has been provided by the U. S. Department of Energy and computational support by the Cornell National Supercomputer Facility.

- 
- [1] R. Bass, *Nuclear Reactions With Heavy Ions* (Springer-Verlag, New York, 1980).
- [2] A. S. Goldhaber and H. H. Heckman, *Annu. Rev. Nucl. Part. Sci.* **28**, 161 (1978).
- [3] W. Zajc, J. A. Bistirlich, R. R. Bossingham, H. R. Bowman, C. W. Clawson, K. M. Crowe, K. A. Frankel, J. G. Ingersoll, J. M. Kurck, C. J. Martoff, D. M. Murphy, J. O. Rasmussen, J. P. Sullivan, E. Yoo, O. Hashimoto, M. Koike, W. J. McDonald, J. P. Miller, and P. Truol, *Phys. Rev. C* **29**, 2173 (1984).
- [4] *Proceedings Corinne '90*, An International Workshop on Particle Correlations and Interferometry in Nuclear Collisions, Nantes, France, 1990, edited by D. Ardouin (World Scientific, Singapore, 1990).
- [5] R. Lacey, N. N. Ajitanand, J. M. Alexander, D. M. De Castro Rizzo, P. DeYoung, M. Kaplan, L. Kowalski, G. LaRana, D. Logan, D. J. Moses, W. E. Parker, G. F. Peaslee, and L. C. Vaz, *Phys. Lett. B* **191**, 253 (1987).
- [6] P. A. DeYoung, M. S. Gordon, Xiu qin Lu, R. L. McGrath, J. M. Alexander, D. M. de Castro Rizzo, and L. C. Vaz, *Phys. Rev. C* **39**, 128 (1989), and references therein.
- [7] A. Elmaani, N. N. Ajitanand, T. Ethvignot, and J. M. Alexander, *Nucl. Instrum. Methods Phys. Res. A* **313**, 401 (1992).
- [8] D. H. Boal, C. K. Gelbke, and B. K. Jennings, *Rev. Mod. Phys.* **62**, 553 (1990); B. K. Jennings, D. H. Boal, and J. C. Shilcock, *Phys. Rev. C* **33**, 1303 (1986), and references therein.
- [9] See, for example, in *Proceedings of the International Workshop on Dynamical Fluctuations and Correlations in Nuclear Collisions, Aussois, France, 1992*, edited by M. Bex, B. Borderie, M. Ploszajczak, J. Richert, P. Schuck, and E. Suraud [*Nucl. Phys. A* **545**, Nos. 1,2 (1992)].
- [10] L. G. Moretto, *Nucl. Phys. A* **247**, 211 (1975); L. G. Moretto and R. P. Schmitt, *Phys. Rev. C* **21**, 204 (1980).
- [11] J. Boger, S. Kox, G. Auger, J. M. Alexander, A. Narayanan, M. A. McMahan, D. J. Moses, M. Kaplan, and G. P. Gilfoyle, *Phys. Rev. C* **41**, R801 (1990); J. Boger, Ph.D. thesis, SUNY Stony Brook, 1991.
- [12] E. Suraud, C. Gregoire, and B. Tamain, *Prog. Nucl. Part. Sci.* **23**, 357 (1989).
- [13] J. Pochodzalla, C. K. Gelbke, W. G. Lynch, M. Maier, D. Ardouin, H. Delagrange, H. Doubre, C. Gregoire, A. Kyanowski, W. Mittig, A. Peghaire, J. Peter, F. Saint-Laurent, B. Zwieglinski, G. Bizard, F. Lefebvres, B. Tamain, J. Quebert, Y. P. Viyogi, W. A. Friedman, and D. H. Boal, *Phys. Rev. C* **35**, 1695 (1987), and references therein.
- [14] B. Jakobsson, B. Noren, A. Oskarsson, M. Westenius, M. Cronqvist, S. Mattson, M. Rydehell, O. Skeppstedt, J. C. Gondrand, B. Khelifaoui, S. Kox, F. Merchez, C. Perrin, D. Rebreyend, L. Westerberg, and S. Pratt, *Phys. Rev. C* **44**, R1238 (1991).
- [15] D. A. Cebra, W. Benenson, Y. Chen, E. Kashy, A. Pradham, A. Van der Molen, G. D. Westfall, W. K. Wilson, D. J. Morrissey, R. S. Tickle, R. Korteling, and R. L. Helmer, *Phys. Lett. B* **227**, 336 (1989).
- [16] D. Rebreyend, F. Merchez, B. Noren, S. Kox, M. Cronquist, J. C. Gondrand, B. Jakobsson, B. Khelifaoui, A. Kristiansson, S. Mattson, O. Oskarsson, C. Perrin, M. Rydehell, O. Skeppstedt, M. Westenius, and L. Westerberg, *Phys. Rev. C* **46**, 2387 (1992).
- [17] M. A. Bernstein, W. A. Friedman, W. G. Lynch, C. B. Chitwood, D. J. Fields, C. K. Gelbke, M. B. Tsang, T. C. Awes, R. L. Ferguson, F. E. Obenshain, F. Plasil, R. L. Robinson, and G. R. Young, *Phys. Rev. Lett.* **54**, 402 (1985); M. A. Bernstein, W. A. Friedman, and W. G. Lynch, *Phys. Rev. C* **29**, 132 (1984), and references therein.
- [18] T. C. Awes, G. Poggi, C. K. Gelbke, B. B. Back, B. G. Glagola, H. Breuer, and V. E. Viola, Jr., *Phys. Rev. C* **24**, 89 (1981).
- [19] H. A. Weidenmuller, *Nucl. Phys. A* **471**, 1 (1987).
- [20] A real nuclear potential was used for  ${}^2\text{H}-{}^2\text{H}$  interactions:  $V(r) = \frac{-V_{ws}}{1 + \exp\left(-\frac{r-r_{ws}}{a_{ws}}\right)}$ , where  $V_{ws} = 50 \text{ MeV}$ ,  $r_{ws} = 5 \text{ fm}$ , and  $a_{ws} = 0.65 \text{ fm}$ .
- [21] W. G. Lynch, C. B. Chitwood, M. B. Tsang, D. J. Fields, D. R. Klesch, C. K. Gelbke, G. R. Young, T. C. Awes, R. L. Ferguson, F. E. Obenshain, F. Plasil, R. L. Robinson, and A. D. Panagiotou, *Phys. Rev. Lett.* **51**, 1850 (1983).
- [22] P. A. DeYoung, C. J. Gelderloos, D. Kortering, J. Sarafa, K. Zienert, M. S. Gordon, B. J. Fineman, G. P. Gilfoyle, X. Lu, R. L. McGrath, D. M. de Castro Rizzo, J. M. Alexander, G. Auger, S. Kox, L. C. Vaz, C. Beck, D. J. Henderson, D. G. Kovar, and M. F. Vineyard, *Phys. Rev. C* **41**, R1885 (1990).
- [23] See, for example, in *Symposium on Nuclear Dynamics and Nuclear Disassembly*, Dallas, Texas, 1989, edited by

- J. B. Natowitz (World Scientific, Singapore, 1989).
- [24] S. E. Koonin, *Phys. Lett.* **70B**, 43 (1977).
- [25] A. Elmaani, N. N. Ajitanand, J. M. Alexander, R. A. Lacey, S. Kox, E. Liatard, F. Merchez, T. Motobayashi, B. Noren, C. Perrin, D. Rebreyend, Tsan Ung Chan, G. Auger, and S. Groult, *Phys. Rev. C* **43**, R2474 (1991); A. Elmaani, Ph.D thesis, SUNY Stony Brook, 1991; A. Elmaani *et al.*, *Phys. Rev. C* (in press).
- [26] M. S. Gordon, R. L. McGrath, J. M. Alexander, P. A. DeYoung, Xiu qin Lu, D. M. de Castro Rizzo, and G. P. Gilfoyle, *Phys. Rev. C* **46**, R1 (1992).
- [27] D. P. Stahel, R. Jahn, G. J. Wozniak, and J. Cerny, *Phys. Rev. C* **20**, 1680 (1979).
- [28] Zhang Ying-ji, Yang Jin-qing, Zhang Jie, and He Jian-hua, *Phys. Rev. C* **45**, 528 (1992).
- [29] A. B. Migdal, *Yad. Fiz.* **16**, 427 (1973) [*Sov. J. Nucl. Phys.* **16**, 238 (1973)].
- [30] P. G. Hansen and B. Jonson, *Europhys. Lett.* **4**, 409 (1987).